Turk Neurosurg, 2021

Original Investigation

DOI: 10.5137/1019-5149.JTN.31996-20.2

Received: 17.08.2020
Accepted: 22.12.2020

Published Online: 06.05.2021

Neurogenesis is Enhanced in Young Rats with Genetic Absence Epilepsy: An Immuno-electron Microscopic Study

Ozlem Tugce CILINGIR-KAYA[1], Cynthia MOORE[2], Charles Kenneth MESHUL[2,3], Duygu GURSOY[4], Filiz ONAT[5], Serap SIRVANCI[1]

[1]Marmara University School of Medicine, Department of Histology and Embryology, Istanbul, Turkey
[2]VA Medical Center/Portland, Research Services, Oregon, USA
[3]Oregon Heath & Science University, Portland, Department of Behavioral Neuroscience, Oregon, USA
[4]Medipol University School of Medicine, Department of Histology and Embryology, Istanbul, Turkey
[5]Marmara University School of Medicine, Department of Medical Pharmacology, Istanbul, Turkey

Corresponding author: Ozlem Tugce CILINGIR-KAYA ✉ tugce.cilingir@marmara.edu.tr

ABSTRACT

AIM: To investigate neurogenesis in both adult and 3-week-old genetic absence epilepsy rats from Strasbourg (GAERS) to determine if newly formed neurons within the dentate gyrus (DG) form synaptic contacts with GABAergic (gamma aminobutyric acid) and glutamatergic nerve terminals and compared to the control (non-GAERS) Wistar rats.

MATERIAL and METHODS: Brain tissue was processed for electron microscopic assessment. Thin sections from the hippocampal DG were double-labelled for anti-GABA or anti-VGLUT1 (vesicular glutamate transporter 1) and anti-doublecortin (DCX) antibodies using immunogold methodology and examined with the transmission electron microscope for morphological changes and to quantify the density of gold labeling.

RESULTS: DCX immunoreactivity was demonstrated within axon terminals, dendrites and somata in all groups. DCX and GABA or VGLUT1 were found to be co-localized in the axon terminals in all groups. We observed that DCX-immunoreactive (-ir) profiles formed synaptic contacts with GABAergic and glutamatergic terminals. The percentage of DCX labeling in dendrites, compared to axons, and the percentage of DCX-ir terminal profiles forming asymmetrical synapses, compared to those forming symmetrical synapses, were increased in all groups compared to the control group. DCX immunoreactivity in the 21-day-old GAERS group was found to be increased compared to the Wistar group.

CONCLUSION: We conclude that newly born neurons are incorporated into the local hippocampal network in both the GAERS and the control Wistar rats. The results suggest that the neurogenesis taking place in the hippocampus may also be involved in the mechanism underlying absence seizures in GAERS.

KEYWORDS: Doublecortin, GABA, VGLUT-1, GAERS, Immunoelectron microscopy

ABBREVIATIONS: ANOVA: Analysis of variance, **CA:** Cornu ammonis, **CCD:** Couple-charged device, **DCX:** Doublecortin, **DG:** Dentate gyrus, **GABA:** Gamma-Aminobutyric Acid, **GAD:** Glutamic acid decarboxylase, **GHB:** Gamma-hydroxybutyrate, **GL:** Granular layer, **-ir:** Immunoreactive, **NEC:** Non-epileptic control, **S.E.M:** Standard error of mean, **SGZ:** Subgranular zone, **TLE:** Temporal lobe epilepsy, **WAG/Rij:** Wistar Albino Glaxo from Rijswijk

Ozlem Tugce CILINGIR-KAYA : 0000-0002-2591-9174
Cynthia MOORE : 0000-0002-9852-8748
Charles Kenneth MESHUL : 0000-0002-3908-0795
Duygu GURSOY : 0000-0001-6698-9032
Filiz ONAT : 0000-0003-0680-4782
Serap SIRVANCI : 0000-0001-7683-4587

INTRODUCTION

Typical generalized absence epilepsy seizures are characterized by a sudden interruption of consciousness associated with bilaterally synchronous spike and wave discharges (SWDs) in the electroencephalography (EEG) (26,44). The role of excessive GABAergic conduction in the cortico-thalamo-cortical circuitry on triggering absence epilepsy has been previously reported (32,49). The hippocampal network was also reported to be altered in this type of epilepsy (24,33,43,44). Genetic absence epilepsy rats from Strasbourg (GAERS) have the features of human absence epilepsy, both neurophysiologically and behaviorally, and also have the EEG characteristics as shown by SWDs; therefore, these animals have been used as an experimental model of absence epilepsy (49).

Interactions between GABA and glutamate, which are the major neurotransmitters in mammalian brain, have played a role in not only normal function and plasticity of the brain, but are impaired in the development of absence epilepsy (35). Glutamate is stored in the presynaptic vesicles through the uptake of this neurotransmitter through the vesicular glutamate transporter (VGLUT) (25). In the hippocampus of adult GAERS, glutamate levels were found to be increased, whereas there was no marked difference in GABA levels was we have previously reported (43,44). However, age-associated alterations in neurotransmission and subsequent effects on the function of the hippocampal glutamate/GABA circuitry have not been thoroughly studied (45).

Neurogenesis occurs during a life-time period in two distinct areas of the adult brain: the subventricular zone of the lateral ventricles and the subgranular zone (SGZ) of the hippocampus (1). Progenitor cells located in the SGZ in the dentate gyrus (DG) migrate to the granular layer (46). These newly migrated cells project their axonal processes into the cornu ammonis (CA)-3 region of the hippocampus (23). It was demonstrated in recent studies that migrated cells join the local neural circuitry and are then transformed into mature and functional neurons (28,50).

In the past few decades, it has been determined that abnormal hippocampal neurogenesis is an important pathophysiological mechanism in the development of temporal lobe epilepsy (TLE) (2,18,28,31,36-38). It has been established that acute seizures or limbic epileptogenesis induce neurogenesis (4,46). Seizures not only affect neurogenesis but also induce migration of neurogenic cells into ectopic regions (46). It has been reported that ectopically migrated cells play a role in the formation of an epileptogenic hippocampal circuitry (2). While recent studies have shown that neurological disorders or injuries cause an increase in neurogenesis, a significant decrease also occurs during ageing (12,51).

DCX, a microtubule associated protein, is transiently expressed in newborns and in migrating neurons, and is also used as a marker for immature neurons. It is synthesized by proliferating progenitor cells and newborn neuroblasts. DCX plays an important role in the regulation and stabilization of microtubules, neural cell migration, and dendritic branching (6,9,21). In the rodent nervous system, expression of DCX is induced by dividing progenitor cells and continues for 30 days, ending after neural maturation (7).

In the present study, we aimed to determine the possible effects of absence epilepsy on neurogenesis in GAERS in comparison to Wistar control rats. Since neurogenesis also depends on the age of the animals, we tested both 21-day- and 3-month-old rats. For this purpose, we investigated for the first time the co-localization of DCX/GABA and DCX/vesicular glutamate transporter-1 (VGLUT1), using post-embedding double immunogold labeling at the electron microscopic level. We investigated whether newborn neural cells, as labeled with DCX, were able to integrate into the local hippocampal circuitry and interact with GABAergic or glutamatergic neurons.

MATERIAL and METHODS

Subjects

21-day-old (Wistar, n=4; GAERS, n=3), 100-150 g and 3-month-old (Wistar, n=5; GAERS, n=5), 250-300 g male Wistar rats and GAERS were used in the study. The animals were housed in a temperature-controlled room (20 ± 3°C) with a 12-h light/dark cycle and fed a standard diet. Full approval of the experimental procedures was obtained from the Animal Care and Use Committee of Marmara University (35.2014. mar).

Electron Microscopy

Animals were deeply anesthetized with ketamine (100 mg/kg) and xylazine hydrochloride (10 mg/kg) and then euthanized by intracardiac perfusion with a fixative solution containing 2.5% glutaraldehyde, 0.5% paraformaldehyde, and 0.1% picric acid in 0.1 M HEPES buffer, pH 7.4. The entire brain was removed and left overnight in the same fixative at 4°C. 300 µm-thick coronal vibratome sections were cut using a a Leica VT 1000S vibratome and DG region of the hippocampus was then dissected. Sections were incubated in 1% osmium tetroxide/1.5% potassium ferricyanide (1:1) for 30 min at room temperature. The samples were then washed several times in deionized water and stained *en block* with aqueous 0.5% uranyl acetate for 30 min at room temperature. The tissue was then dehydrated in a graded series of ethanol, cleared in propylene oxide, and embedded in Epon 812 for 24 h at 60°C. Semi-thin sections (1 µm) were cut on a ultramicrotome (Leica Ultracut EM UC7, Germany), stained with toluidine blue and viewed with the light microscope (Olympus BX51, Japan) to ensure proper orientation. The tissue was then thin sectioned (80 nm), collected on 100 mesh formvar-coated nickel grids, and air dried for 3–4 h. Double immunogold labeling was carried out with two different sized gold particles for determining the localization of DCX/GABA and DCX/VGLUT1.

Double Immunogold Labeling

Grids containing the tissue sections were washed in TBST pH 7.6 (0.1% Triton X-100, 0.9% NaCl, 0.05 M Tris buffer, pH 7.6), then incubated overnight at room temperature in anti-GABA (Sigma A2052, 1:10,000 in TBST pH 7.6) or anti-VGLUT1 antibody (Synaptic System, Cat #: 135 303, 1:1,000,000 in

TBST pH 7.6). After washing with TBST pH 7.6 and TBST pH 8.2, respectively, sections were incubated in 6 nm gold conjugated secondary goat anti-rabbit IgG antibody (Jackson ImmunoResearch, Cat #: 111-195-144, 1:50 in TBST pH 8.2) for 90 min at room temperature. Sections were then washed in TBST pH 7.6 and exposed to paraformaldehyde vapor at 80ºC in order to inactivate any unbound secondary antibody for the second labeling. After washing in TBST pH 7.6, sections were incubated overnight at room temperature in anti-DCX antibody (Abcam, Cat #: ab18723, 1:200 in TBST pH 7.6). Sections were then incubated in 18 nm gold conjugated secondary goat-anti rabbit IgG antibody (Jackson ImmunoResearch, Cat #: 111-215-144, 1:50 in TBST pH 8.2) for 90 min at room temperature. To account for any possible background labeling due to the secondary antibody, the primary antibody was omitted in all experimental groups, in which we found no labelin.

For the electron microscopic observations, all sections were examined and photographed using a JEOL JEM-1400 transmission electron microscope, which was attached to a CCD camera (#V600 AMT, Woburn, MA, USA). All of the experimental procedures are illustrated in Figure 1.

Quantitative Analysis

Ten micrographs were taken from the DG of each animal. The areas of DCX positive axons and dendrites, both presynaptic and postsynaptic, excluding the somata, were measured and the number of 18 nm gold particles were counted. The density of DCX immunoreactivity was calculated by dividing the number of gold particles by the area of the profile (particles/μm^2). The same method was applied for GABA and VGLUT-1 immunoreactive (-ir) profiles, which included 6 nm gold particles. The number of gold particles and the area of the profiles was calculated by using Image-ProPlus 6.0 software. We also calculated the percentage of axons and dendrites which were either single-labeled for DCX or dual-labeled for DCX/GABA and DCX/VGLUT1. DCX-ir axons and dendrites were counted in 10 photographs in each animal and a percentage was obtained by dividing the number of axons by the total number of profiles, and a similar calculation was also carried out for the dendrites. The type of synaptic contact associated with the DCX-ir profiles was classified as either asymmetrical or symmetrical, and the percentage of such contacts was then calculated. In all of the analyses, the number of gold particles within the mitochondria and the area of the mitochondria were not included in the final nerve terminal density analysis.

Statistical Analysis

GraphPad Prism 7.02 was used for the statistical analysis. The data were analyzed using Students' unpaired *t*-test when two groups were compared, and a one-way ANOVA, followed by Tukey's test for multiple comparisons test when more than two groups were compared. The data are shown as the mean±S.E.M. All statistical analyses was considered significant when $p<0.05$.

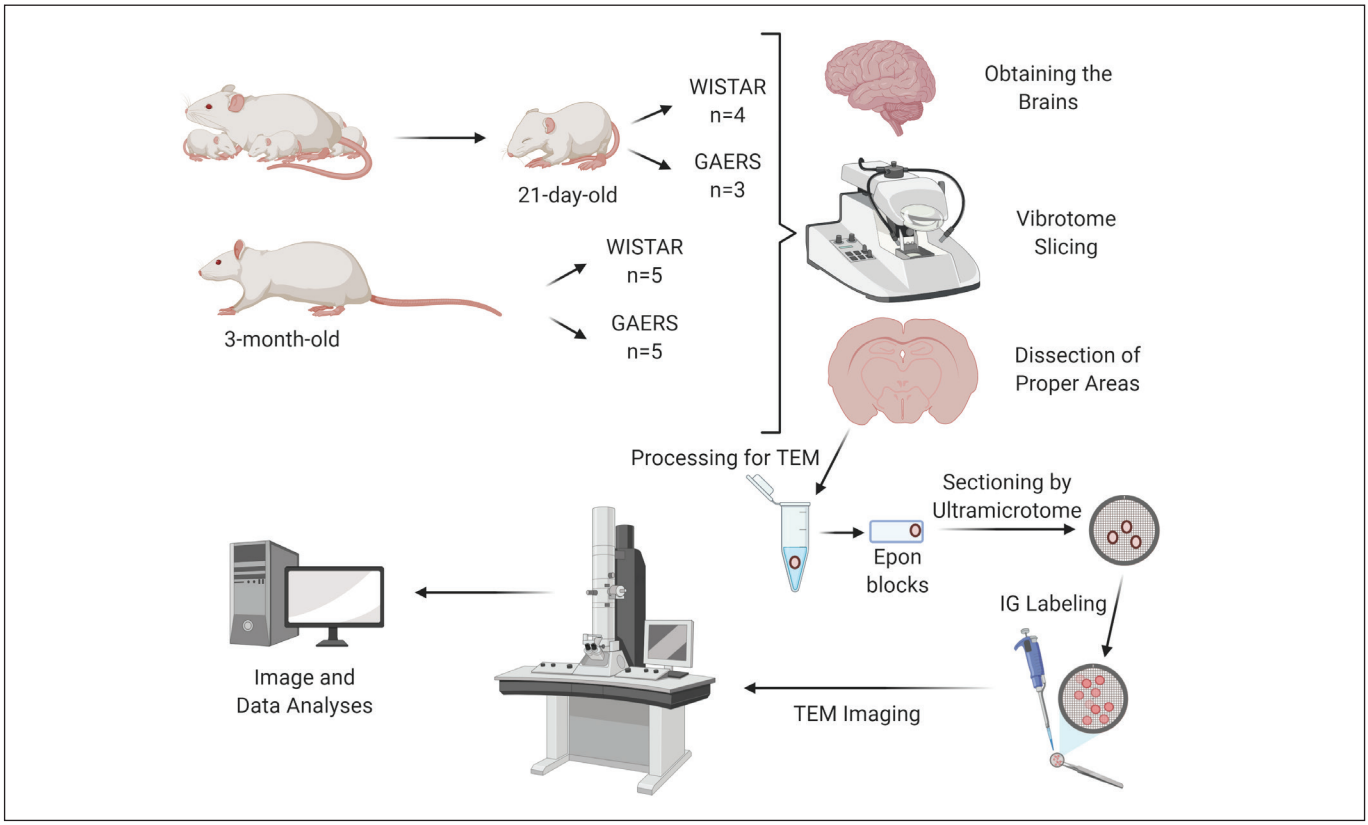

Figure 1: Scheme of the experimental procedures.

RESULTS

Morphological Findings

In all groups, DCX-ir cells were seen mostly in the SGZ, but were also apparent in the granular cell layer and the hilus. The majority of DCX-ir cells were observed as having a round nucleus. DCX immunolabeling was localized to axon terminals, dendrites and somata. DCX labeling was especially detected in the cytoplasm and the cell processes. While some of DCX-ir cells did not have fully developed processes, some of these cells contained dendritic processes (Figure 2A). Some of the DCX (+) somata contained an indented nucleus, and some nerve terminals were immunolabeled for GABA (Figure 2B). There were also dual-labeled axon terminals and dendrites for DCX and GABA, which were observed making synaptic contacts (Figure 2C, D).

In the 21-day-old Wistar group, we determined the extent of DCX immunoreactivity located within on the heterochromatin, near and/or directly associated with on the ribosomes, and in the pre- and post-synaptic regions (Figure 3A, C). Postsynaptic DCX (+) dendrites were seen to making an asymmetrical type of synaptic contact, with the presynaptic terminal being an axon terminal (Figure 3E).

In the 21-day-old GAERS group, DCX-ir cell bodies were observed-making synaptic contacts with GABAergic axon terminals (Figure 3B) and DCX-ir dendrites with immunonegative axons (Figure 3D). DCX immunoreactivity was also observed in mossy fiber terminals, and some of these terminals contained a high density of GABA immunogold labeling (Figure 3F).

In the 3-month-old Wistar group, DCX immunoreactivity was found associated with heterochromatin and the ribosomes in the somata. GABA (+) nerve terminals were observed making synaptic contact with these DCX positive somata (Figure 4A). Dual labeling for GABA and DCX was apparent within dendrites and axon terminals. These double-labeled axon terminals were found making synaptic-like connections with

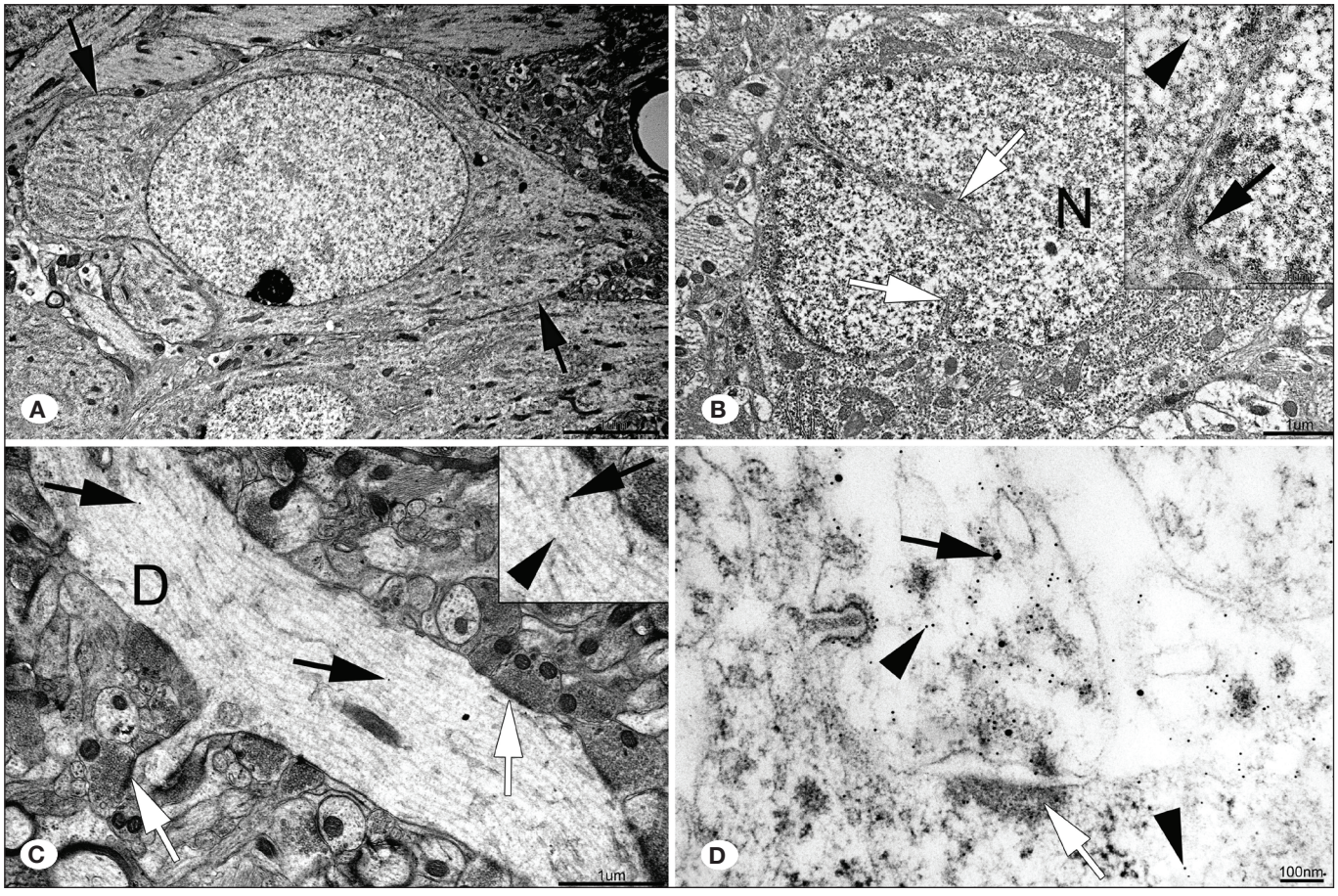

Figure 2: A) A newly born cell with two processes (arrow) which are not fully developed from the 3-month-old GAERS group. **B)** A cell with an indented (white arrow) nucleus (N), which is double-labeled both for DCX (arrow) and GABA (arrowhead) from the 3-month-old Wistar control group. **C)** Synaptic contacts (white arrow) on a double-labeled DCX- (arrow) and GABA-ir (arrowhead) dendrite (D) from the 21-day-old Wistar control group. **D)** An asymmetrical synaptic-like contact between a double-labeled DCX (arrow) and GABA-ir (arrowhead) nerve terminal and another GABA (+) (arrowhead) profile with a post-synaptic density (white arrow) from the 21-day-old Wistar control group.

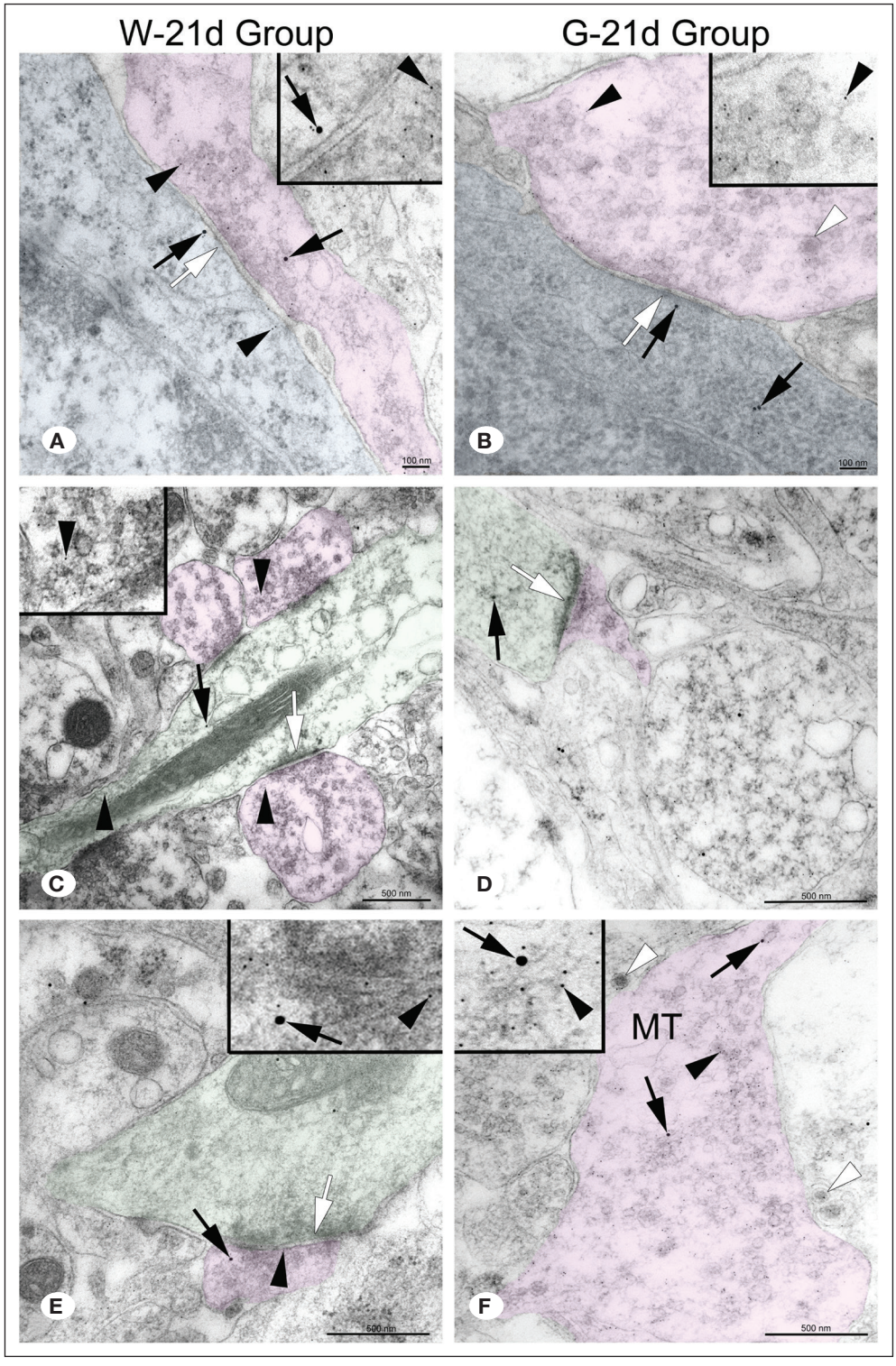

Figure 3: Micrographs of DCX and GABA double-labeling from the 21-day-old groups. Blue area: cell body; pink area: axon; green area: dendrite; MT: mossy terminal. **A)** 21-day-old Wistar group. Arrow: 18 nm gold particles indicating DCX immunoreactivity; arrowhead: 6 nm gold particles indicating GABA immunoreactivity; white arrow: synapse-like contact. **B)** From the 21-day-old Wistar group. Arrow: DCX immunoreactivity; arrowhead: GABA immunoreactivity; white arrow: synaptic contact. **C)** From the 21-day-old Wistar group. Arrow: DCX immunoreactivity; arrowhead: GABA immunoreactivity. **D)** From the 21-day-old GAERS group. Arrow: DCX immunoreactivity; arrowhead: GABA immunoreactivity in the mossy terminal; white arrowhead: dense core vesicle; white arrow: synaptic contact, MT: mossy terminal. **E)** From the 21-day-old group. Arrow: DCX immunoreactivity; white arrow: synaptic contact. **F)** From the 21-day-old GAERS group. Arrow: DCX immunoreactivity; arrowhead: GABA immunoreactivity; white arrowhead: dense core vesicle.

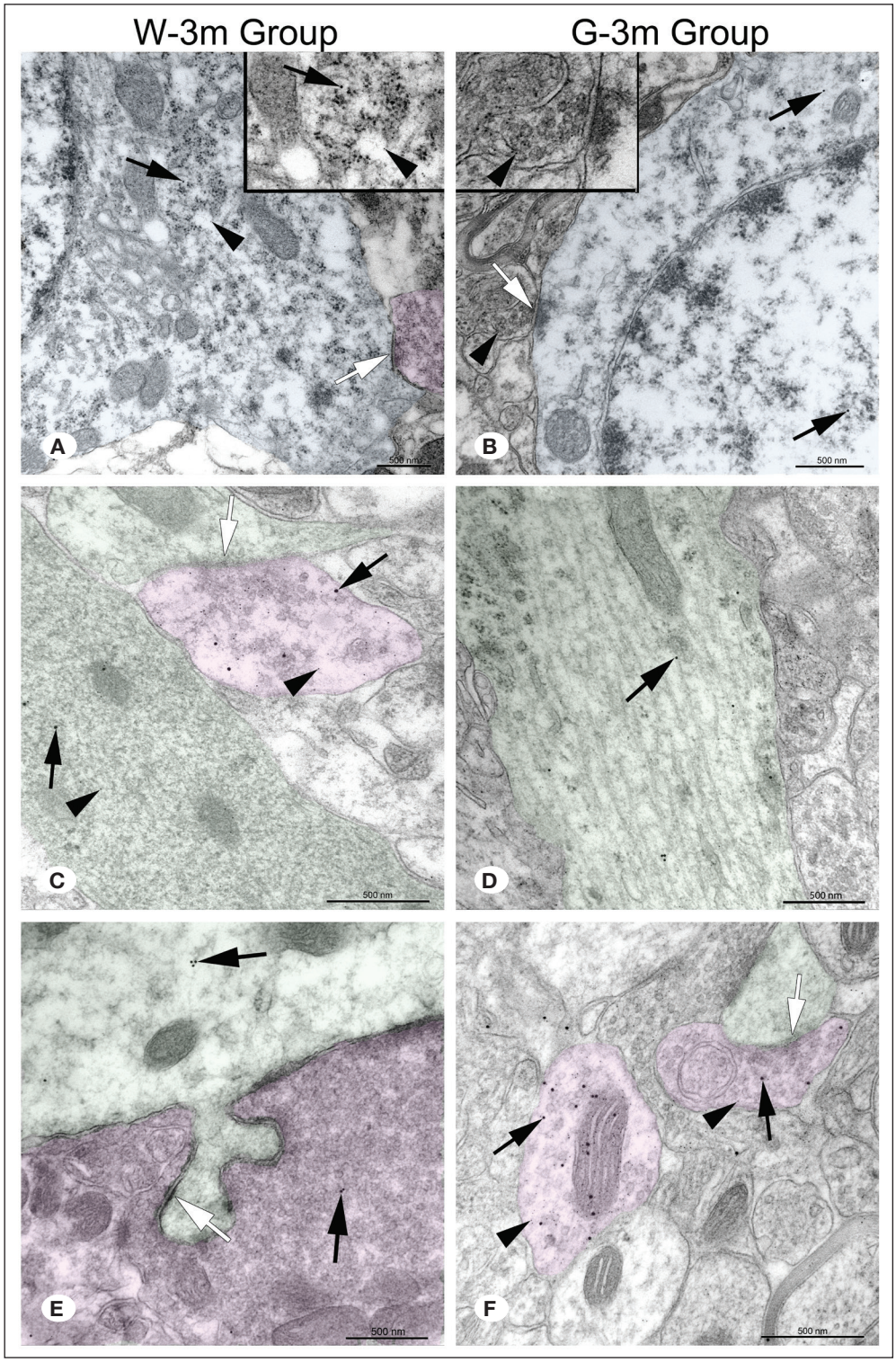

Figure 4: Electron photomicrographs of DCX and GABA double-immuno-gold labeling in the 3-month-old groups. Blue area: cell body; pink area: axon; green area: dendrite; MT: mossy terminal. **A)** From the 3-month-old Wistar group. Arrow: 18 nm gold particles indicating DCX immunoreactivity; arrowhead: 6 nm gold particles indicating GABA immunoreactivity; white arrow: synaptic contact. **B)** From the 3-month-old Wistar group. Arrow: DCX immunoreactivity; arrowhead: GABA immunoreactivity; white arrow: synaptic contact. **C)** From the 3-month-old Wistar group. Arrow: DCX immunoreactivity; white arrow: synaptic contact; MT: mossy terminal. **D)** From the 3-month-old GAERS group. Arrow: DCX immunoreactivity; arrowhead: GABA immunoreactivity; white arrow: synapse-like contact. **E)** From the 3-month-old GAERS group. Arrow: DCX immunoreactivity; white arrow: synaptic contact; white arrowhead: dense core vesicle. **F)** From the 3-month-old GAERS group. Arrow: DCX immunoreactivity; arrowhead: GABA immunoreactivity; white arrow: synaptic contact.

immune-negative profiles (Figure 4C). DCX positive mossy fiber terminals were observed making synaptic contact with DCX positive dendrites (Figure 4E).

In the 3-month-old GAERS group, DCX immunoreactivity was observed in the somata near and/or on the ribosomes and heterochromatin (Figure 4B). DCX-ir dendrites were observed to have a low density of GABA immunoreactivity (Figure 4D), whereas DCX (+) axon terminals were found to have a higher density of GABA immuno-gold labeling (Figure 4F).

VGLUT1 immunoreactivity was also seen in the DCX positive or negative nerve terminals that contained spherical vesicles. In addition, DCX/VGLUT1 double-labeled profiles were observed making synaptic contact with both immunonegative or immunopositive structures that were positive for VGLUT1 and/or DCX (Figure 5A-D).

Statistical Data

DCX immunoreactivity was found to be higher in the 21-day-old GAERS group compared to the 21-day-old Wistar group and this difference was statistically significant (p=0.03) (Figure 6A). However, there was no significant difference in the density of DCX immunoreactivity in the 3-month-old GAERS rats compared to 3-month-old Wistar controls. Besides, the percentage of DCX (+) dendrites compared to DCX (+) axons in all groups was found to be significantly increased (p<0.001) (Figure 6B). The percentage of dual labeled GABA and DCX axon terminals was significantly increased in the 21-day-old GAERS group compared to that of the dual labeled dendrites (p=0.01) (Figure 6D). There was no difference in the percentage of GABA and DCX-ir dual labeled profiles and in the density of GABA immuno-gold labeling between the groups (Figure 6C, E). We then classified the synaptic contacts as to whether they were either a DCX (+) single or dual labeled and if the contact was as symmetrical or asymmetrical. We observed that the synaptic contact associated with the DCX-ir profiles were primarily asymmetrical compared to that of being a symmetrical, and this difference was statistically significant (p<0.001) (Figure 6F). There was no difference in VGLUT1 immunoreactivity in DCX-ir positive or immunonegative profiles between the groups (Figure 6G, H).

DISCUSSION

In the present study, we are the first to report postembed double immunogold labeling was used to localize DCX/GABA and DCX/VGLUT1 immunoreactivity at the electron microscopic level in Wistar rats and GAERS. Our results indicate that both

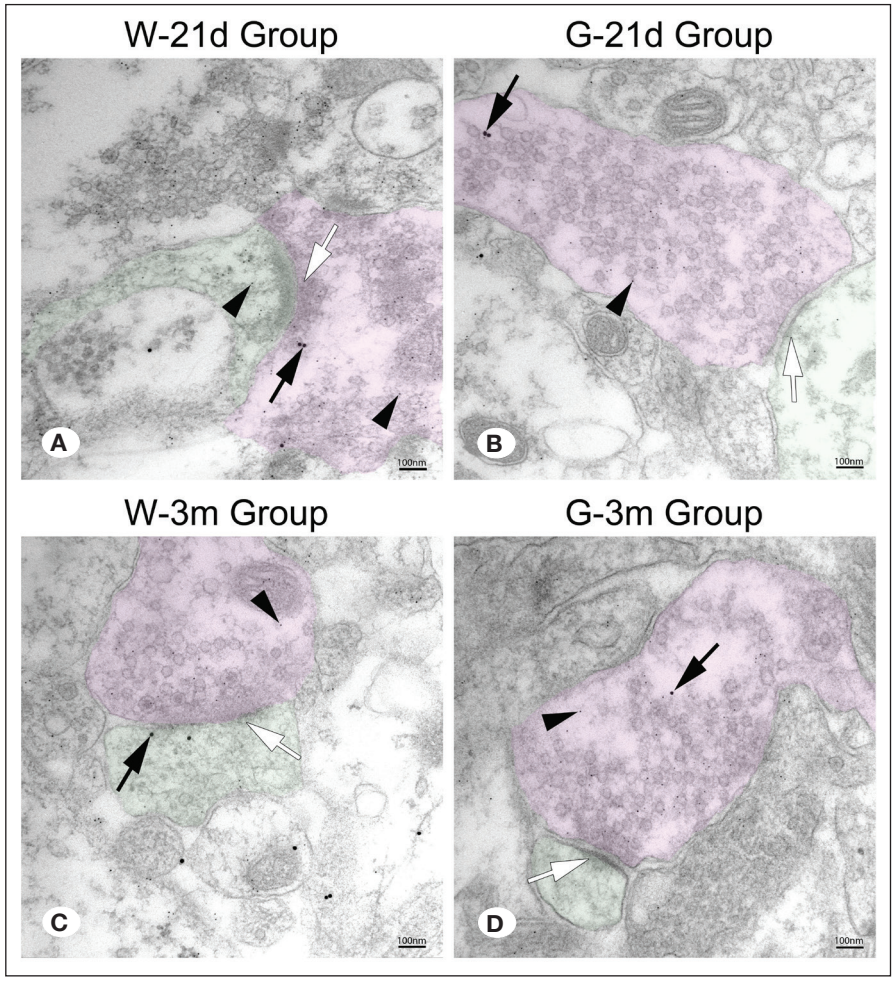

Figure 5: Electron photomicrographs of DCX and VGLUT1 double immuno-gold labeling in all groups. Arrow: DCX immunoreactivity; arrowhead: VGLUT1 immunoreactivity; white arrow: postsynaptic density.

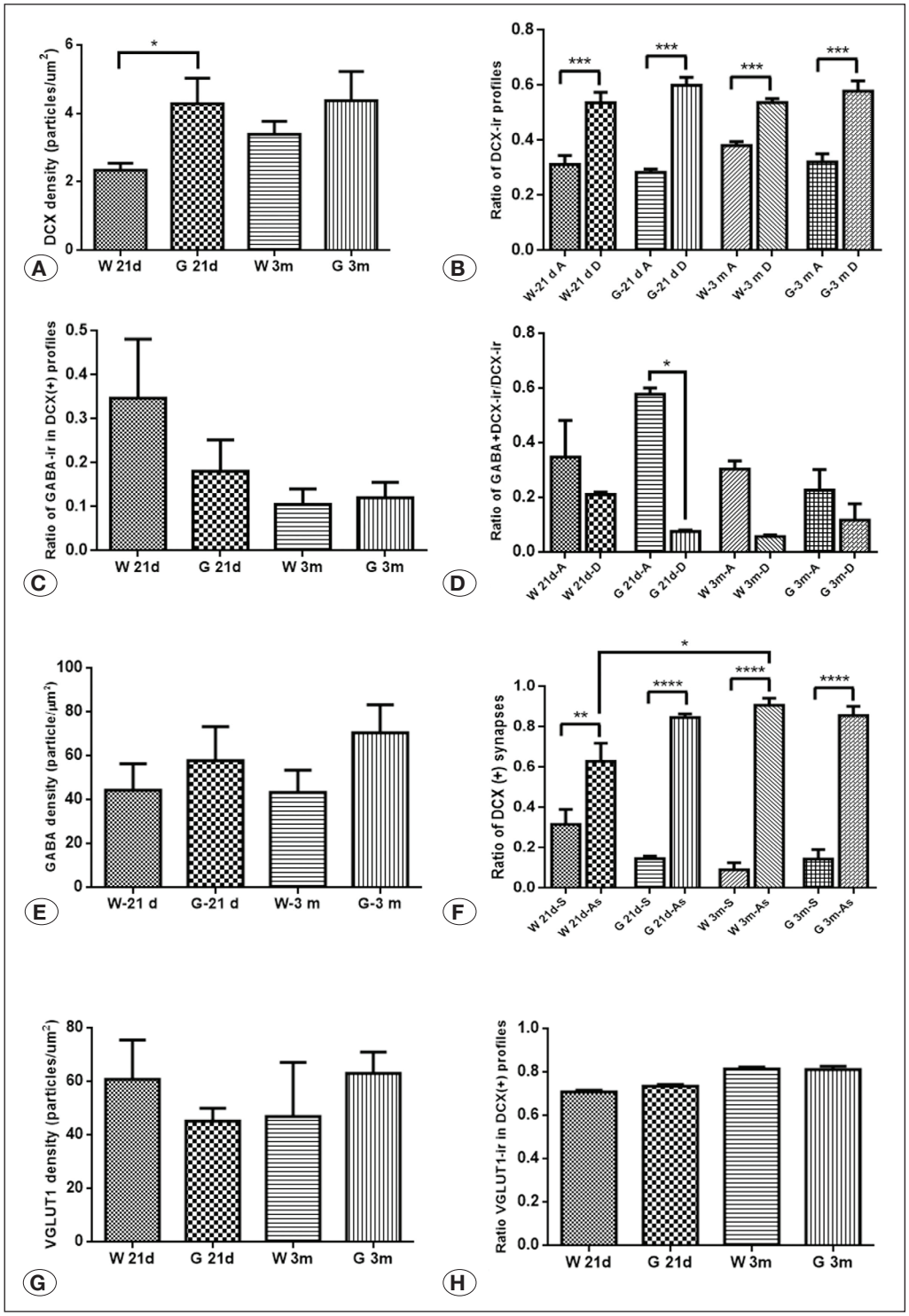

Figure 6: A) Density of 18 nm gold particles indicating DCX immunoreactivity. (Unpaired t-test, *p=0,0340). **B)** Percentage of DCX-ir axons or dendrites in all DCX (+) profiles. (One way ANOVA, *** p<0.001, DFn=7, DFd=28 and the F value=18.13). **C)** Percentage of dual-labeled profiles for DCX and GABA in all DCX (+) profiles. **D)** Percentage of dual-labeled axons or dendrites for DCX and GABA in all DCX (+) profiles. (One-way ANOVA, *p=0.0147, ***p=0.0008; DFn=7, DFd=12 and the F-value=4.189). **E)** Density of 6 nm gold particles as an indicator of GABA labeling. **F)** Comparison of DCX-ir profiles associated the specific type of synpatic contact. (One-way ANOVA, *p<0.05; **p<0.01; ****p < 0.0001; DFn=7, DFd=32 and the F-value= 48.31). W 21d: Wistar 21-day-old group, W 3m: Wistar 3-month-old group, G 21d: GAERS 21-day-old group, G 3m: GAERS 3-month-old group. A: Axon, D: dendrite, S: Symmetrical synaptic contact, As: asymmetrical synaptic contact. **G)** Density of 6 nm gold particles as an indicator of VGLUT1 labeling. **H)** Percentage of dual-labeled profiles for DCX and VGLUT1 in all DCX (+) profiles.

local and newly formed GABAergic and glutamatergic neurons cells within the DG make synaptic contact with DCX-ir newly born cells in both immature and adult control and in GAER epileptic rats. This suggests that immature neurons contribute to the neuronal circuitry in both control and absence epileptic pups and in adult rats.

We observed DCX-ir cells localized in the SGZ, which is consistent with previous work reported by Shapiro et al. (40). The authors also stated that newly born cells might show dendritic processes, similar to those shown in our study. In parallel with the report by Herrick et al., we observed DCX immunoreactivity associated with the heterochromatin within the nucleus and on the ribosomes within the cytoplasm (19). In the present study, most of the DCX-ir neurons had the morphology of granule cells with regular and round nuclei, and this finding was also consistent with previous studies (19,41). However, some DCX-ir cells showed the features of GABAergic inhibitory cells, i.e., with the soma having an indented nucleus and the axon terminals being double-labeled with both DCX and GABA. This result is consistent with previous reports that 14% of the newly born cells in the DG of adult rats are composed of GABAergic basket cells (22). The percentage of DCX-ir dendritic profiles was greater more than that of DCX-ir axons in all groups. We hypothesize that these results may be due to the fact that DCX is a microtubule-associated protein (13) and the dendrites have more dynamic microtubule structures in contrast to that of the axons (3). In the neurons of vertebrates, the ratio of microtubules to neurofilaments is significantly higher in dendrites than axons (27). Newly born neurons of the adult DG strongly express DCX (18), and this may be related to the formation and maturation of the dendritic tree in neurons that are undergoing differentiation (8).

It is known that DG granule cells express GABAergic markers at early stages of development and this GABAergic phenotype might be related to the trophic effects of GABA (15). GABA released from mossy fiber terminals is excitatory during the first 7 days of postnatal development and then inhibitory until 22-23rd days; thereafter no GABA is normally released from mossy fiber terminals (17,34). However, under abnormal conditions such as seizures, mossy fiber terminals of adult animals may then release GABA. At this point in time, mossy fiber terminals regulate the maturation of pyramidal cells until dendrite and spine formation is completed (17). Besides, axons which originate from dentate granule cells are recognized as having a dual GABAergic and glutamatergic phenotype (16). We previously observed deregulation of the metabolism of GLU and its membrane transporters in the cortex and/or thalamus of young GAERS prior to the development of seizures (10,11), suggesting an early impairment of GLU neuro-circuitry, which may be involved in the genesis of this pathology (48). GABA and glutamic acid decarboxylase (GAD) in the hippocampus of both adult Wistar control rats and GAERS strain has been reported at the electron microscopic level (42-44), with no differences found in either GABA and GAD density. Similarly, in the current study, there was no difference in GABA density in the hippocampal inhibitory nerve terminals between the GAERS and Wistar control rats. Our observations showed that mossy fiber terminals in the 21-day-old animals made synapse-like connections and contained GABA. Mossy fiber terminals in the 3-month-old group were also GABA-ir positive. This finding, consistent with previous reports, suggests that GABA found within in mossy fiber terminals of 21-day-old control and epileptic animals may be functional and have inhibitory effects on other neurons within the hilus. Furthermore, this GABA immunolabeling found in 21-day-old rats may also be acting as a trophic factor, as previously reported (17,34).

In the current study, there was no difference in the density of VGLUT1 labeling between the adult and young GAERS and Wistar rats. VGLUT1 immunoreactivity and protein levels remained constant across all age groups, starting at postnatal month 1 (PM1; adolescent), PM6, PM12 (adult group), PM18 and PM24 (the aged groups). These results suggest that VGLUT1 may be less susceptible to the aging process (20). In line with the previous study of Bergersen et al., we observed the colocalization of GABA and glutamate in the same terminals (5).

We show in the current study that DCX-ir cells formed synaptic connections, with our finding consistent with previous reports (19,47). We observed that DCX-ir profiles made asymmetrical compared to symmetrical synaptic contacts more often and this difference was statistically significant. This finding is consistent with a previous study demonstrating that most of the newly born neurons are making excitatory synaptic contacts, while a small number of the contacts have inhibitory/symmetrical features (29). In addition, the ratio of GABA (+)/DCX dual-labeled profiles was significantly smaller compared to non-GABAergic profiles in all groups.

It was shown in previous studies that limbic epileptogenesis with extended seizures stimulated hippocampal neurogenesis (4,30). In kainate and pilocarpine models of TLE, DG cell proliferation was shown to increase significantly after a few days following a long latent period (14,30). Scott et al. (39) used the gamma-hydroxybutyrate (GHB) model for typical and AY-9944 model for atypical absence seizures to investigate neurogenesis in adult rats and then compared the results with that of a kindling mode. Rats with absence epilepsy did not show any significant difference from the controls in terms of newly born cells. However, neurogenesis was shown to increase in the kindling model. The present study showed that the density of DCX immunolabeled cells significantly increased in the 21-day-old GAERS group compared to 21-day-old Wistar control group, which may indicate enhanced neurogenesis in this model of genetic absence epilepsy. However, there was no difference in the density of DCX positive neurons between the 3-month-old GAERS and 3-month-old Wistar groups, a finding which is in line with the study of Scott et al. (39).

Our results showed that DCX and GABA or VGLUT-1 could be co-expressed within the same neuron and that these newly born nerve cells are capable of making synaptic contact with other neural elements in both the GAERS and control Wistar animals. This is the first report of neurogenesis in the GAERS strain. Our study contributes to the epilespy literature by revealing the relationship between this GAERS model of epilepsy and neurogenesis.

In summary, double immunogold (postembed) labeling to localize both method for DCX and GABA/VGLUT-1 at the electron microscopic level was applied for the first time in the hippocampus of both GAERS and Wistar control rats. Increased DCX immunoreactivity in 21-day-old GAERS suggests that there is enhanced neurogenesis in the hippocampus of these animals. This 21 day old time period corresponds to the moment before the appearance of spike-and-wave discharges in this strain. Therefore, we suggest that the hippocampus may also be involved in the mechanism(s) underlying absence epilepsy in this GAERS strain of rats.

CONCLUSION

These results reveal that the most important factors affecting hippocampal neurogenesis in epilepsy are the type and mechanism of seizure and epileptic discharges.

ACKNOWLEDGEMENTS

This study is a part of Ozlem Tugce Cilingir's doctorate thesis research. It was supported by the Research Fund of the Marmara University [grant number SAG-C-DRP-100413-0112, 2013]; Merit Review [grant numbers #BX001643 and #BX000552] to CKM, Department of Veterans Affairs Biomedical Laboratory Research and Development, OR, United States (U.S.). The contents do not represent the views of the U.S. Department of Veterans Affairs or the United States Government. The overseas assignment at the Portland VA Medical Center as a part of this doctorate thesis study was supported by Turkish Council of Higher Education according to law number 2547/39.

REFERENCES

1. Altman J, Das GD: Autoradiographic and histological evidence of postnatal hippocampal neurogenesis in rats. J Comp Neurol 124:319-335, 1965
2. Avanzini G, Franceschetti S: Cellular biology of epileptogenesis. The Lancet Neurology 2:33-42, 2003
3. Avila J: Microtubule Proteins. USA: CRC Press Florida, 1989
4. Bengzon J, Kokaia Z, Elmer E, Nanobashvili A, Kokaia M, Lindvall O: Apoptosis and proliferation of dentate gyrus neurons after single and intermittent limbic seizures. Proceedings of the National Academy of Sciences of the United States of America 94:10432-10437, 1997
5. Bergersen L, Ruiz A, Bjaalie JG, Kullmann DM, Gundersen V: GABA and GABAA receptors at hippocampal mossy fibre synapses. Eur J Neurosci 18:931-941, 2003
6. Brown JP, Couillard-Despres S, Cooper-Kuhn CM, Winkler J, Aigner L, Kuhn HG: Transient expression of doublecortin during adult neurogenesis. J Comp Neurol 467:1-10, 2003
7. Brown MN: GABA synthesis in developing hippocampus: SNAT1 surfaces as a dynamic regulator of inhibitory synaptic transmission. Vanderbilt University, 2010
8. Cohen D, Segal M, Reiner O: Doublecortin supports the development of dendritic arbors in primary hippocampal neurons. Developmental Neuroscience 30:187-199, 2008
9. Deuel TA, Liu JS, Corbo JC, Yoo SY, Rorke-Adams LB, Walsh CA: Genetic interactions between doublecortin and doublecortin-like kinase in neuronal migration and axon outgrowth. Neuron 49:41-53, 2006
10. Dutuit M, Didier-Bazès M, Vergnes M, Mutin M, Conjard A, Akaoka H, Belin MF, Touret M: Specific alteration in the expression of glial fibrillary acidic protein, glutamate dehydrogenase, and glutamine synthetase in rats with genetic absence epilepsy. Glia 32:15-24, 2000
11. Dutuit M, Touret M, Szymocha R, Nehlig A, Belin MF, Didier-Bazès M: Decreased expression of glutamate transporters in genetic absence epilepsy rats before seizure occurrence. J Neurochem 80:1029-1038, 2002
12. Galvan V, Jin K: Neurogenesis in the aging brain. Clin Interv Aging 254):605-610, 2007
13. Gleeson JG, Lin PT, Flanagan LA, Walsh CA: Doublecortin is a microtubule-associated protein and is expressed widely by migrating neurons. Neuron 23:257-271, 1999
14. Gray WP, Sundstrom LE: Kainic acid increases the proliferation of granule cell progenitors in the dentate gyrus of the adult rat. Brain Res 790:52-59, 1998
15. Gutierrez R: The GABAergic phenotype of the "glutamatergic" granule cells of the dentate gyrus. Prog Neurobiol 71:337-358, 2003
16. Gutierrez R: The dual glutamatergic-GABAergic phenotype of hippocampal granule cells. Trends in neurosciences 28:297-303, 2005
17. Gutierrez R, Romo-Parra H, Maqueda J, Vivar C, Ramirez M, Morales MA, Lamas M: Plasticity of the GABAergic phenotype of the "glutamatergic" granule cells of the rat dentate gyrus. J Neurosci 23:5594-5598, 2003
18. Hattiangady B, Rao MS, Shetty AK: Chronic temporal lobe epilepsy is associated with severely declined dentate neurogenesis in the adult hippocampus. Neurobiol Dis 17:473-490, 2004
19. Herrick SP, Waters EM, Drake CT, McEwen BS, Milner TA: Extranuclear estrogen receptor beta immunoreactivity is on doublecortin-containing cells in the adult and neonatal rat dentate gyrus. Brain Res 1121:46-58, 2006
20. Jung HY, Yoo DY, Park JH, Kim JW, Chung JY, Kim DW, Won MH, Yoon YS, Hwang IK: Age-dependent changes in vesicular glutamate transporter 1 and 2 expression in the gerbil hippocampus. Mol Med Rep 17:6465-6471, 2018
21. Kronenberg G, Reuter K, Steiner B, Brandt MD, Jessberger S, Yamaguchi M, Kempermann G: Subpopulations of proliferating cells of the adult hippocampus respond differently to physiologic neurogenic stimuli. J Comp Neurol 467:455-463, 2003
22. Liu S, Wang J, Zhu D, Fu Y, Lukowiak K, Lu YM: Generation of functional inhibitory neurons in the adult rat hippocampus. J Neurosci 23:732-736, 2003
23. Markakis EA, Gage FH: Adult-generated neurons in the dentate gyrus send axonal projections to field CA3 and are surrounded by synaptic vesicles. J Comp Neurol 406:449-460, 1999
24. Nehlig A, Vergnes M, Boyet S, Marescaux C: Local cerebral glucose utilization in adult and immature GAERS. Epilepsy Res 32:206-212, 1998

25. Omote H, Moriyama Y: Vesicular neurotransmitter transporters: An approach for studying transporters with purified proteins. Physiology (Bethesda) 28:39-50, 2013
26. Onat FY, van Luijtelaar G, Nehlig A, Snead OC 3rd: The involvement of limbic structures in typical and atypical absence epilepsy. Epilepsy Res 103:111-123, 2013
27. Palay SL, Chan-Palay V: Cerebellar Cortex: Cytology and Organization. Springer, 1974
28. Parent JM, Elliott RC, Pleasure SJ, Barbaro NM, Lowenstein DH: Aberrant seizure-induced neurogenesis in experimental temporal lobe epilepsy. Annals of Neurology 59:81-91, 2006
29. Parent JM, von dem Bussche N, Lowenstein DH: Prolonged seizures recruit caudal subventricular zone glial progenitors into the injured hippocampus. Hippocampus 16:321-328, 2006
30. Parent JM, Yu TW, Leibowitz RT, Geschwind DH, Sloviter RS, Lowenstein DH: Dentate granule cell neurogenesis is increased by seizures and contributes to aberrant network reorganization in the adult rat hippocampus. J Neurosci 17:3727-3738, 1997
31. Pirttilä TJ, Lukasiuk K, Håkansson K, Grubb A, Abrahamson M, Pitkänen A: Cystatin C modulates neurodegeneration and neurogenesis following status epilepticus in mouse. Neurobiol Dis 20(2):241-253, 2005
32. Richards DA, Lemos T, Whitton PS, Bowery NG: Extracellular GABA in the ventrolateral thalamus of rats exhibiting spontaneous absence epilepsy: A microdialysis study. J Neurochem 65:1674-1680, 1995
33. Richards DA, Morrone LA, Bowery NG: Hippocampal extracellular amino acids and EEG spectral analysis in a genetic rat model of absence epilepsy. Neuropharmacology 39:2433-2441, 2000
34. Safiulina VF, Fattorini G, Conti F, Cherubini E: GABAergic signaling at mossy fiber synapses in neonatal rat hippocampus. J Neurosci 26:597-608, 2006
35. Samardzic J, Jadzic D, Hencic B, Jancic J, Svob Strac D: GABA/Glutamate Balance: A key for normal brain functioning. In: Samardzic J (ed), GABA and Glutamate - New Developments in Neurotransmission Research. IntechOpen, 2018
36. Scharfman HE, Goodman JH, Sollas AL: Granule-like neurons at the hilar/CA3 border after status epilepticus and their synchrony with area CA3 pyramidal cells: Functional implications of seizure-induced neurogenesis. J Neurosci 20:6144-6158, 2000
37. Scharfman HE, Sollas AE, Berger RE, Goodman JH, Pierce JP: Perforant path activation of ectopic granule cells that are born after pilocarpine-induced seizures. Neuroscience 121:1017-1029, 2003
38. Scharfman HE, Sollas AL, Smith KL, Jackson MB, Goodman JH: Structural and functional asymmetry in the normal and epileptic rat dentate gyrus. J Comp Neurol 454:424-439, 2002
39. Scott BW, Chan KF, Wong G, Ahmed M, Chieverton L, Liu RR, Wood J, Burnham WM: Cytogenesis in the adult rat dentate gyrus is increased following kindled seizures but is unaltered in pharmacological models of absence seizures. Epilepsy & Behavior 18(3):179-185, 2010
40. Shapiro LA, Korn MJ, Shan Z, Ribak CE: GFAP-expressing radial glia-like cell bodies are involved in a one-to-one relationship with doublecortin-immunolabeled newborn neurons in the adult dentate gyrus. Brain Res 1040:81-91, 2005
41. Shapiro LA, Ribak CE: Newly born dentate granule neurons after pilocarpine-induced epilepsy have hilar basal dendrites with immature synapses. Epilepsy Res 69:53-66, 2006
42. Sirvanci S, Canillioglu Y, Akakin D, Midillioglu S, Yildiz SD, Onat F, San T: Glutamic acid decarboxylase immunoreactivity in the mossy fiber terminals of the hippocampus of genetic absence epileptic rats. Turk Neurosurg 21:499-503, 2011
43. Sirvanci S, Meshul CK, Onat F, San T: Glutamate and GABA immunocytochemical electron microscopy in the hippocampal dentate gyrus of normal and genetic absence epilepsy rats. Brain Res 1053:108-115, 2005
44. Sirvanci S, Meshul CK, Onat F, San T: Immunocytochemical analysis of glutamate and GABA in hippocampus of genetic absence epilepsy rats (GAERS). Brain Research 988:180-188, 2003
45. Stephens ML, Quintero JE, Pomerleau F, Huettl P, Gerhardt GA: Age-related changes in glutamate release in the CA3 and dentate gyrus of the rat hippocampus. Neurobiology of Aging 32:811-820, 2011
46. Taupin P: BrdU immunohistochemistry for studying adult neurogenesis: Paradigms, pitfalls, limitations, and validation. Brain Research Reviews 53:198-214, 2007
47. Toni N, Laplagne DA, Zhao C, Lombardi G, Ribak CE, Gage FH, Schinder AF: Neurons born in the adult dentate gyrus form functional synapses with target cells. Nature Neuroscience 11:901-907, 2008
48. Touret M, Parrot S, Denoroy L, Belin MF, Didier-Bazes M: Glutamatergic alterations in the cortex of genetic absence epilepsy rats. BMC Neuroscience 8:69, 2007
49. van Luijtelaar G, Depaulis A: Genetic Models of Absance Epilepsy in the Rat. In: Pitkänen A, Schwartkroin PA, Moshé SL (ed), Models of Seizures and Epilepsy. Elsevier Academic Press, 2006: 233-248
50. van Praag H, Schinder AF, Christie BR, Toni N, Palmer TD, Gage FH: Functional neurogenesis in the adult hippocampus. Nature 415(6875):1030-1034, 2002
51. Yu S, Yang S, Holsboer F, Sousa N, Almeida OF: Glucocorticoid regulation of astrocytic fate and function. PloS one 6:e22419, 2011